Propulsion and Power Research 2012;1(1):71–77

http://ppr.buaa.edu.cn/

Propulsion and Power Research

www.sciencedirect.com

ORIGINAL ARTICLE

Effect of cross-flow direction of coolant on film cooling effectiveness with one inlet and double outlet hole injection

Guangchao Li*, Chaolin Wu, Wei Zhang, Zhihai Kou, Dawei Peng

Liaoning Key Laboratory of Advanced Technology for Aeronautical Propulsion System, Aeroengine and Energy Engineering College, Shenyang Aerospace University, Shenyang, Liaoning 110136, China

Received 19 May 2012; accepted 24 September 2012
Available online 20 December 2012

KEYWORDS

Aerospace propulsion system;
Turbine blade;
Film cooling;
Cross-flow;
Numerical simulation

Abstract In order to study the effect of cross-flow directions of an internal coolant on film cooling performance, the discharge coefficients and film cooling effectiveness with one inlet and double outlet hole injections were simulated. The numerical results show that two different cross-flow directions of the coolant cause the same decrease in the discharge coefficients as that in the case of supplying coolant by a plenum. The different proportion of the mass flow out of the two outlets of the film hole results in different values of the film cooling effectiveness for three different cases of coolant supplies. The film cooling effectiveness is the highest for the case of supplying coolant by the plenum. At a lower blowing ratio of 1.0, the film cooling effectiveness with coolant injection from the right entrance of the passage is higher than that from the left entrance of the passage. At a higher blowing ratio of 2.0, the opposite result is found.

1. Introduction

The temperature of a gas turbine inlet is increased year by year in order to output larger power, and it has become higher than the melting point of the material. The blade must be effectively cooled to ensure that the engine works normally. Film cooling of an engine is one means of effective cooling, and the shapes of film holes significantly affect the film cooling effectiveness. Interest in the film cooling characteristics of different shaped

*Corresponding author.
E-mail address: ligc706@yahoo.com.cn (Guangchao Li)

Peer review under responsibility of National Laboratory for Aeronautics and Astronautics, China.

ELSEVIER Production and hosting by Elsevier

2212-540X © 2012 National Laboratory for Aeronautics and Astronautics. Production and hosting by Elsevier B.V. All rights reserved.
http://dx.doi.org/10.1016/j.jppr.2012.10.006

hole injections has increased since the beginning of the 1990s. In the case of the same blowing ratios, the lower velocity of coolant in film hole outlets can decrease the miscibility between the coolant and the gas, thereby increasing the film cooling effectiveness. Thus, the film hole outlets are expanded into different shapes such as cones, fans, and dust-pans [1–3]. However, these shaped holes are difficult to machine. The design of film holes based on a cylindrical hole has recently been developed, including the addition of an axon ridge at the upstream of the film hole [4] and a transverse slot on the film hole outlet [5]. The structures of the shaped holes can be easily machined, and the film cooling characteristics are improved compared to the cylindrical hole injections because of the weaker mixing and the better spanwise diffusion. A more effective cooling area was achieved when injecting through a compound angle because of the good spanwise diffusion of the coolant [6,7].

The injections from the two adjacent film holes interact with each other to change the structure of the vortex outside of the film hole, resulting in better coverage of the coolant on the surface [8]. Heidmann and Ekkad [9] designed a hole with an anti-vortex film cooling concept by injecting coolant through two small symmetrical holes to mitigate the effect of the counter-vortex pair. The various orientations of the small holes have a significant effect on film performance. However, the orientation angles of the small holes are limited by the hole pitch. When the orientation angle is large, the hole pitch must be increased to ensure that the neighbouring small holes do not intersect. The symmetry of the two small holes also reduces the effect of the compound angle injection. The trunk-branch hole has only one branch hole injection, which improves the effect of the compound angle injection.

This paper focuses on the effect of cross-flow directions of the coolant on the characteristics of film cooling with one inlet and double outlet holes. The branch hole of one inlet and two outlet holes play a role in the fixed values of the compound angle. The relative directions of the cross-flow of the internal coolant and the branch hole angle cause various vortices in and out of the film hole, resulting in a marked effect on the proportion of the mass flow rate out of the two outlets. Therefore, the film cooling effectiveness has different characteristics [10].

2. Numerical simulation method [11]

2.1. Computational domain and the grids

Figure 1 shows the computational domain including the gas passage, film hole, and internal passage of the coolant. The film hole consists of the trunk hole with injection into the mainstream direction and the branch hole with injection into the compound angle. The

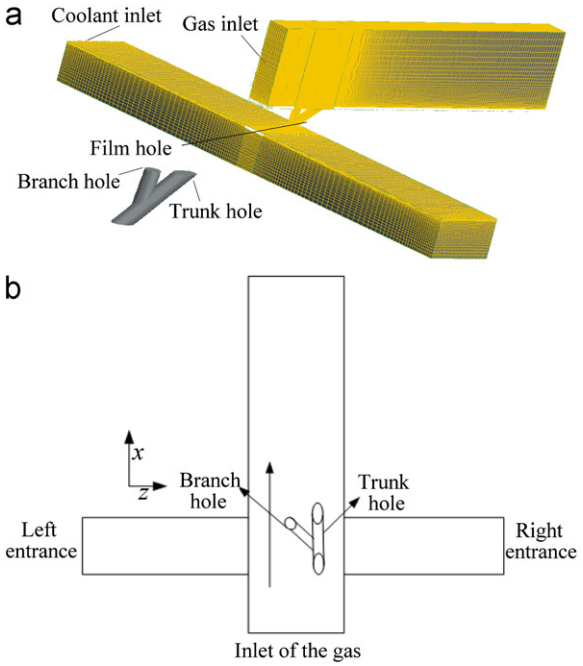

Figure 1 Grids and the geometric model. (a) Computational domain and the grids and (b) relative location angle of the film hole and the coolant passage entrance.

periodic condition was used for the gas passage in the radial direction. The coordinate origin is located in the centre of the film hole outlet. Figure 1(b) shows the directions of the x-axis and z-axis. The y-axis is perpendicular to the x–z section. The relative directions of the coolant cross-flow and positive z-axis are also shown in Figure 1(b). The injection from the branch hole deflects to the left entrance of the internal cooling passage.

The grids of the mainstream tunnel are generated as three separate regions in the stream-wise direction. The unstructured grids are generated in the middle domain neighbouring the film cooling holes, and the structured grids are generated in the other two domains. The grids lengthen in the positive y-axis direction. The first layer grids close to the cooled surface are 0.1 mm in the positive y-axis direction, resulting in the corresponding $y+$ from 1 to 10 depending on the various locations of the computational domain. The grids of the film cooling holes and the plenum are generated respectively. The grid number of the entire domain is approximately 1.2×10^6.

The detailed definitions of the geometric parameters are shown in Figure 2, and the relative values of these parameters are listed in Table 1. The trunk hole angle with respect to the surface in the mainstream direction is 30°. The branch hole is similar to the compound angle injection. The angle of the branch hole with respect to the surface is 60°. The branch hole also has an orientation angle of 45°. The ratio of the branch hole diameter to the trunk hole diameter is 0.9. The smaller branch

hole diameter is easily machinable considering the manufacturing error. The axis lines of the two holes intersect at the location of one trunk hole diameter from the hole inlet.

2.2. Parameter definitions and computation conditions

The blowing ratio is defined as

$$M = \frac{\rho_c u_c}{\rho_\infty u_{loc}} \tag{1}$$

The discharge coefficient is defined as

$$C_D = \frac{m_r}{m_i} = \frac{m_r}{(\pi \times d^2/4)\sqrt{2\rho_c(P_2^* - P_e)}} \tag{2}$$

The cross-flow velocity ratio is defined as

$$V_r = \frac{u_{cross}}{u_c} \tag{3}$$

here ρ_c is the secondary flow density; u_c, the average velocity of the secondary flow through the cylindrical section in the film hole inlet; ρ_∞, the mainstream density; u_{loc}, the velocity of the mainstream in the film hole outlet without the film flow; m_r, the mass flow rate through the film hole and m_i, the ideal mass flow rate through the film hole. The parameter d is the diameter of the trunk hole; P_2^*, the total pressure of the film hole inlet; P_e, the static pressure of the film hole outlet; and u_{cross}, the velocity of the coolant in the internal cooling passage.

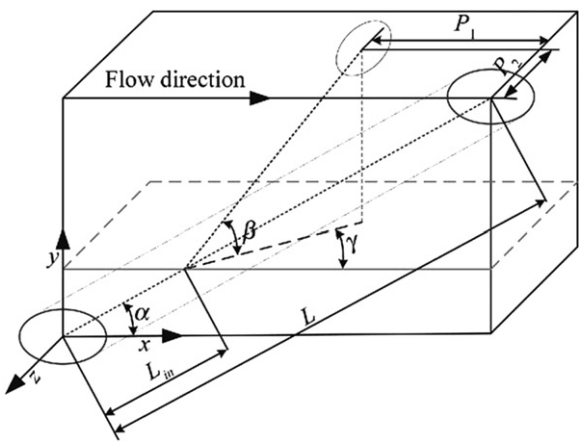

Figure 2 Definition of geometric parameters.

The cooling effectiveness is defined as

$$\eta = \frac{T_{aw} - T_\infty}{T_c - T_\infty} \tag{4}$$

The dimensionless temperature is defined as

$$\theta = (T - T_\infty)/(T_c - T_\infty) \tag{5}$$

here, T_{aw} is the adiabatic temperature; T_∞, the temperature of the mainstream; and T_c, the temperature of the secondary flow set on the entrance of the coolant.

The spanwise-averaged film cooling effectiveness is calculated as

$$\eta_{ave} = \frac{1}{n}\sum_{i=1}^{n}\eta_i \tag{6}$$

here, n is the number of the spanwise grids at the same location of x/d and η_i is the film cooling effectiveness of the local spanwise grid.

The velocity at the gas inlet is 15 m/s, and the Reynolds number based on the diameter of the film hole inlet and the gas velocity is 9600. The velocity at the internal cooling passage inlet is 15 m/s. The blowing ratios are 1.0, 1.5, and 2.0. The velocity ratios are 1.0, 0.67, and 0.5, depending on the different blowing ratios. Table 2 lists the three cross-flow directions of the internal coolant. Case 1 is the baseline.

The temperature of the coolant was maintained at 30 K above the mainstream according to the test conditions. The relative density ratio of the coolant to the mainstream was 0.91. The cooled surface was treated as the isothermal surface, so the temperature of the cooling surface is the adiabatic temperature T_{aw}. The periodic condition was used for the gas passage in the radial direction.

2.3. Computation method and turbulence model

The film cooling problem was modelled by the compressible Navier–Stokes equation and the energy equations that are valid for a thermally and calorically perfect gas. The effects of turbulence were modelled

Table 1 Detailed parameters of the film cooling hole.

α/(deg.)	The angle of the trunk hole in the mainstream direction	30
β/(deg.)	The angle of the branch hole with respect to the surface	60
γ/(deg.)	The orientation angle of the branch hole	45
L/d	The ratio of the length of the trunk to the diameter of the hole	6
L_{in}/d	The ratio of the entry length of the trunk to the diameter of the hole	1.5
P/d	The ratio of the distance of the neighbouring holes to the diameter of the hole	3
P_1/d	The ratio of the distance of the mainstream direction between the two outlets to the diameter of the hole	3
P_2/d	The ratio of the spanwise distance between the two outlets to the diameter of the hole	0.9

Table 2 Three cross-flow directions of the internal coolant.

Case 1	From the plenum
Case 2	From the left entrance of the passage
Case 3	From the right entrance of the passage

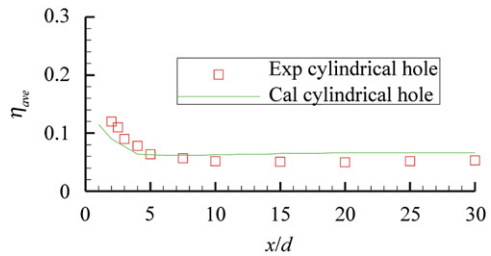

Figure 3 Comparison of experimental data and numerical results.

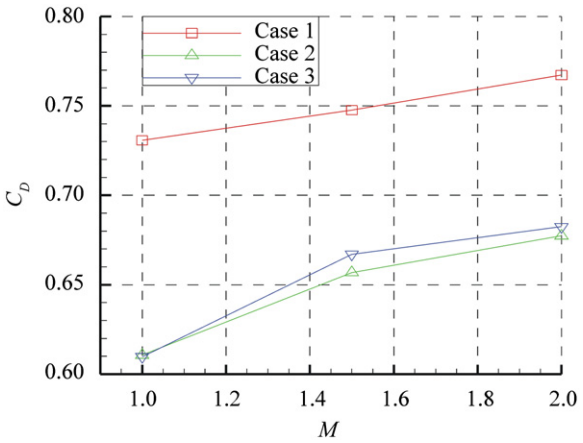

Figure 4 Effect of the cross-flow direction on the discharge coefficients.

using the two-equation realizable k–ε model. Solutions to the governing equations were obtained using Version 6.3.26 of the Fluent code. Since only steady-state solutions were of interest, the SIMPLE algorithm was used. The fluxes at the cell faces representing advection and diffusion were interpolated using second-order upwind differences. For all computations, iterations were continued until all residuals for all equations plateaued to ensure that convergence to steady state was reached. At convergence, the normalized residuals were always less than 10^{-6} for the continuity equation and the three components of the velocity, less than 10^{-8} for the energy, and less than 10^{-5} for the turbulence quantities.

The chosen turbulence model significantly affects the numerical results. The realizable k–ε turbulence model and the enhanced wall function were used to solve the Navier–Stokes equation. The film cooling effectiveness from the realizable k–ε turbulence model agrees well with the experimental results in Ref. [12]. The spanwise-averaged film cooling effectiveness with a standard cylindrical hole calculated in this study is consistent with the experimental data for the same flow cases and geometries in the literature [13], as shown in Figure 3. The largest difference between the experimental data and the numerical results is less than 10%. This indicates that the realizable k–ε turbulence model and the generated grids can be used for calculating the film cooling effectiveness.

3. Results and discussion

3.1. Effect of cross-flow direction on the flow performance

Figure 4 shows a comparison of the discharge coefficients for the cases of three different cross-flow directions of the internal coolant. The discharge coefficients of the film hole for the case of supplying the coolant by the plenum are more than those of the film hole with the internal coolant cross-flow from 15% to 20%.

The additive flow loss is found at the film hole inlet in the presence of the cross-flow because the flow vector turns 90°, resulting in the small discharge coefficients as compared to the case of the plenum. A pressure lift is also found across the hole inlet in the tunnel because of the coolant bleed, but it insufficiently overcomes the flow loss caused by the turning of the coolant. The value of the pressure lift increases with an increase in the blowing ratios, resulting in a decrease in the difference among the discharge coefficients for the three different coolant supplies.

The effect of the cross-flow directions on the discharge coefficient is less than 3%. In Ref. [14], although the discharge coefficients are significantly decreased by the cross-flow, the increasing compound angle of the film hole results in a small change in the flow loss of the film hole outlet and an increase in the flow loss of the film hole inlet. In this paper, the film hole inlets in the two different cross-flow directions have the same cross-flow angle of 90°, which explains the similar discharge coefficients.

Figure 5 shows the ratios of the mass flow through the trunk hole to the total mass flow through the film hole entrance. There is a weak dependence of the proportion of the mass flow on the blowing ratios, but a strong dependence on the coolant cross-flow directions. In the absence of the cross-flow, the proportions of the mass flow out of the two outlets only differ by 20%, and the ratio of the mass flow is 0.4. In the presence of the cross-flow, the proportion of the mass flow out of the two outlets is significantly different. The coolant is mainly injected into the gas through the branch hole, and the ratio of the mass flow is less than 0.2 when the coolant enters the internal cooling passage from the left entrance. However, the coolant is mainly

injected into the gas through the trunk hole, and the mass flow ratio is 0.7 when the coolant enters the internal cooling passage from the right entrance. The results of the discharge coefficients and discharge proportion show that the internal coolant cross-flow directions have a significant effect on the discharge proportion of the two outlets but a weak effect on the discharge coefficients of the film hole.

Figure 6 shows the vector downstream of the film hole vertical to the direction of the mainstream at a blowing ratio of 1.0. Geometries of the vortices similar to those from the compound angle injection are found when supplying the coolant from the left entrance into the passage, as shown in Figure 6(a). The vortices are lifted off the surface and entrain the gas into the sub-layer of the coolant, resulting in a low film cooling effectiveness. A better attachment of the vortex on the surface is found when supplying the coolant from the right entrance and the plenum, as shown in Figure 6(b and c). The scales of the vortices are smallest when supplying the coolant from the right entrance.

Figure 6 also shows the contour of the dimensionless temperature downstream of the film hole vertical to the direction of the mainstream at a blowing ratio of 1.0. A high and uniform dimensionless temperature of the fluid close to the surface is found when supplying the coolant by the plenum. A narrow band of high dimensionless temperature is found when supplying the coolant from the right entrance into the passage compared to the case of supplying the coolant by the plenum. The narrowest band of the high dimensionless temperature is found when supplying the coolant from the left entrance into the passage.

Figure 7 shows the vector downstream of the film hole vertical to the gas mainstream direction at a blowing ratio of 2.0. The scales of the vortices increase when supplying the coolant from the left entrance into the passage and by the plenum compared to the case of a blowing ratio of 1.0. However, similar scales of the vortices are found when supplying the coolant from the right entrance into the passage.

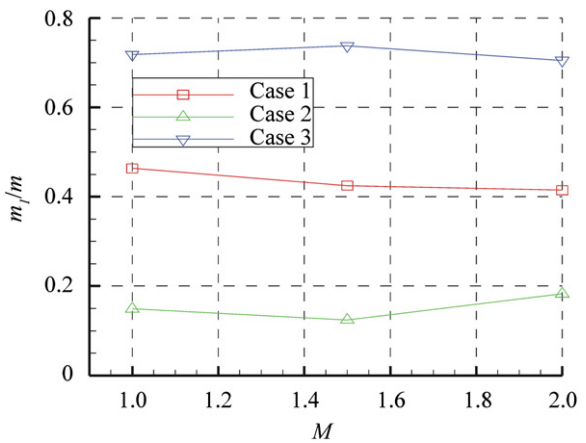

Figure 5 Effect of the internal cross-flow directions on the ratios of the mass flow out of the two outlets.

3.2. *Effect of cross-flow directions on the film cooling effectiveness*

Figure 8 shows the local cooling effectiveness contour in the three different coolant-flow cases at a blowing ratio of 1.0. The local film cooling effectiveness contours in two different cross-flow directions weakly skewed on the negative z-axis. In the absence of the cross-flow, although there is a compound angle injection, the film cooling effectiveness contour hardly skewed on the z-axis. This implies that the inclination of the contour is mainly generated by the cross-flow, not the compound angle injection. The injections from the branch hole of No. 1 and from the trunk hole of No. 2 give a band of high cooling effectiveness in the two different cross-flow directions. The injections from the two outlets of the same hole give a band of high cooling effectiveness, resulting in the largest area covered with the coolant. As the scales of the vortices increase as a result of supplying the coolant from the left entrance, the bandwidth of the high film cooling effectiveness quickly narrows in the mainstream direction compared to the two other cases of coolant supply.

Figure 9 shows the local cooling effectiveness contour in the three different coolant-flow cases at a blowing ratio of 2.0. The cooling effectiveness contour significantly skewed to the negative z-axis compared to the contour at a blowing ratio of 1.0. The high, continuous contours of the film cooling effectiveness are found beyond $x/d=5$ in the cases

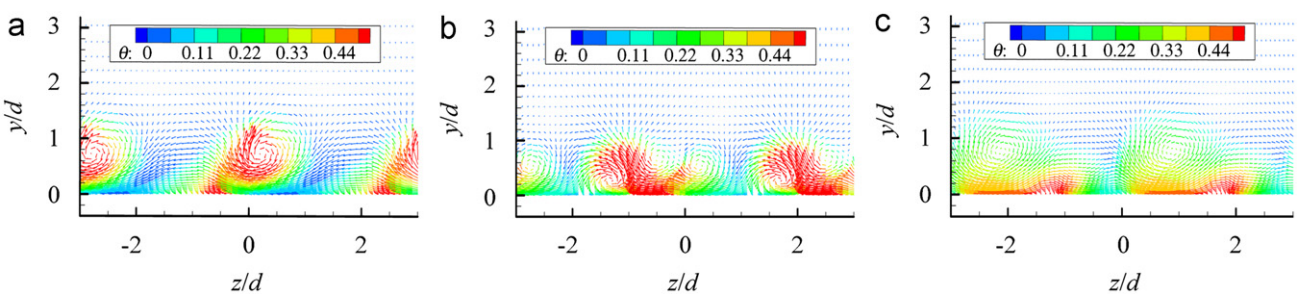

Figure 6 Vector vertical to the mainstream ($x/d=5$, $M=1.0$). (a) Coolant from the left entrance, (b) coolant from the right entrance and (c) coolant from the plenum.

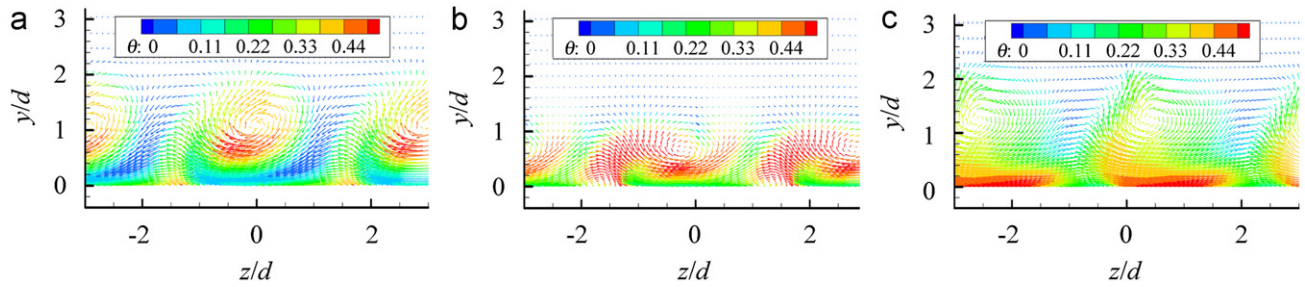

Figure 7 Vector vertical to the mainstream ($x/d=5$, $M=2.0$). (a) Coolant from the left entrance, (b) coolant from the right entrance and (c) coolant from the plenum.

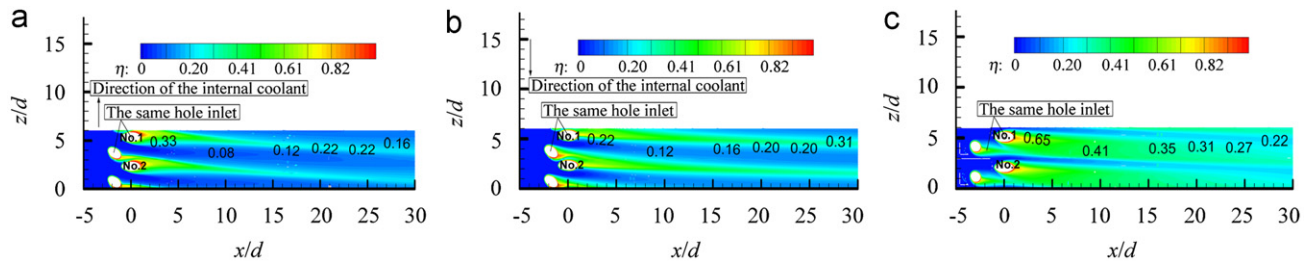

Figure 8 Effect of cross-flow directions on the contour of the local film cooling effectiveness at $M=1.0$. (a) Coolant from the left entrance, (b) coolant from the right entrance and (c) coolant from the plenum.

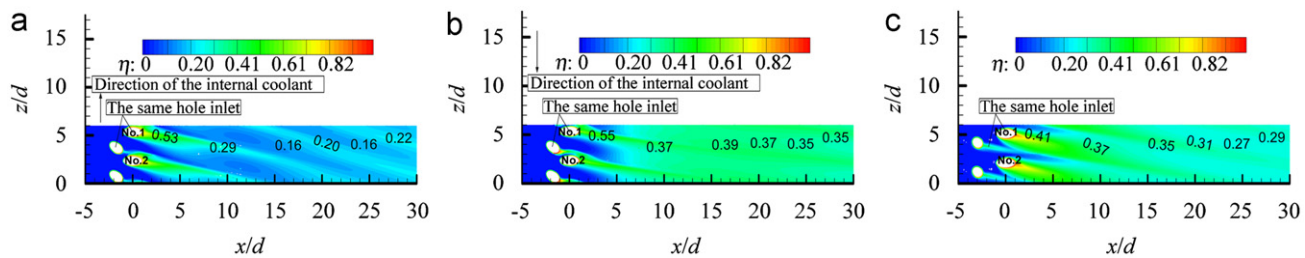

Figure 9 Effect of cross-flow directions on the contour of the local film cooling effectiveness at $M=2.0$. (a) Coolant from the left entrance, (b) coolant from the right entrance and (c) coolant from the plenum.

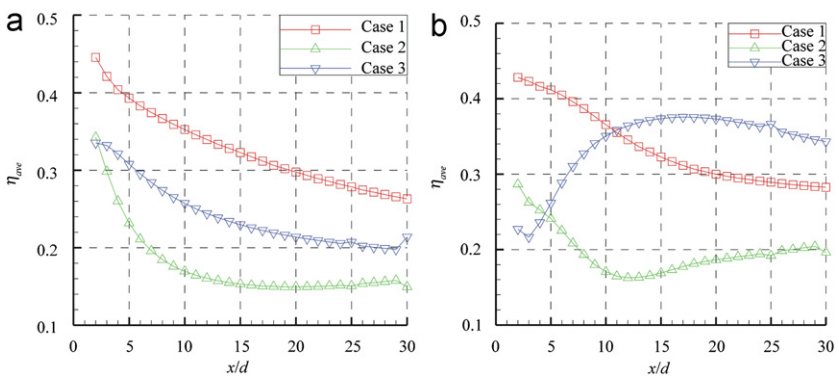

Figure 10 Effect of cross-flow directions on the spanwise average film cooling effectiveness. (a) $M=1.0$ and (b) $M=2.0$.

of supplying the coolant from the left entrance and the plenum.

Figure 10 shows the effect of the three different cross-flow directions on the spanwise average film cooling effectiveness at blowing ratios of 1.0 and 2.0. The film cooling effectiveness from supplying the coolant by the plenum is the highest at a blowing ratio of 1.0. The values of cooling effectiveness of the two different cross flows have a weak difference at the first measured point of $x/d=2$, but with an increase in x/d, the effect of the cross-flow

directions on the cooling effectiveness becomes increasingly significant. The cooling effectiveness of supplying the coolant from the right entrance is higher by approximately 30% than the cooling effectiveness of supplying the coolant from the left entrance at $x/d>5$. Figure 6 shows the vector at $x/d=5$ downstream of the hole outlet for the cases of the three different coolant supplies at a low blowing ratio of 1.0. The vortices for the case of the entrance of the coolant from the left are larger compared to the entrance of the coolant from the right, resulting in entraining more coolant. The vortex is broken into several small vortices in the case of the entrance of the coolant from the right, resulting in the short length of the coolant penetrating into the gas.

At a higher blowing ratio of 2.0, the cooling effectiveness of the coolant from the right entrance is lower than the cooling effectiveness of the coolant from the left entrance at the region of $x/d<4$. But with an increase in x/d, the effect of the cross-flow directions on the cooling effectiveness decreases and equalizes at $x/d=5$. With an increase in x/d, the differences in the values of film cooling effectiveness in the cases of the two different cross flows become significant. Figure 7 shows the vector at $x/d=5$ downstream of the hole outlet for the cases of the three different coolant supplies at a high blowing ratio of 2.0. Several small vortices are found for the case of the coolant from the right entrance, resulting in high film cooling effectiveness compared to the case of the coolant from the left entrance.

4. Conclusion

This paper reports the effect of the internal coolant cross-flow direction on the film cooling performance by numerical simulation, and the following conclusions are drawn:

(1) Coolant cross-flow inflow directions significantly affect the discharge proportion of two outlets from one inlet and double outlet hole.
(2) When the coolant is supplied by the plenum, the discharge coefficients of the film hole are greater than that with the cross-flow of the internal coolant. Two different coolant cross flows weakly affect the discharge coefficients but significantly affect the discharge proportion of the two outlets.
(3) The film cooling effectiveness is the highest when the coolant is supplied by the plenum. At a lower blowing ratio of 1.0, the film cooling effectiveness with coolant injection from the right entrance of the passage is higher than that from the left entrance of the passage. At a higher blowing ratio of 2.0, the opposite result is found.

Acknowledgement

The authors gratefully acknowledge the support of the Aeronautical Science Foundation of China (2010ZB54004).

References

[1] H.R. Zhu, D.C. Xu, S.L. Liu, Effect of hole shape on film cooling effectiveness, Acta Aeronautica et Astronautica Sinica 16 (5) (2002) 75–78 (in Chinese).
[2] H.R. Zhu, D.C. Xu, T. Guo, S.L. Liu, Effect of film cooling hole shape on heat transfer, Journal of Aerospace Power 16 (4) (2001) 360–364 (in Chinese).
[3] H.R. Zhu, D.C. Xu, S.L. Liu, The experimental study in the effect of film cooling hole shape on discharge coefficients, Journal of Propulsion Technique 19 (1) (2002) 42–45 (in Chinese).
[4] S. Na, T.I. Shih, Increasing adiabatic film-cooling effectiveness by using an upstream ramp, ASME Journal of Heat Transfer 129 (2007) 464–471 April.
[5] Y. Lu, A. Dhungel, S.V. Ekkad, Effect of trench width and depth on film cooling from cylindrical holes embeded in trenches, ASME GT2007-27388, 2007.
[6] R.J. Goldstein, P. Jin, Film cooling downstream of a row of discrete holes with compound angle, ASME Journal of Turbomachinery 123 (2) (2001) 222–230.
[7] I.S. Jung, J.S. Lee, Effect of orientation angles on film cooling over a flat plate: boundary layer temperature distributions and adiabatic film cooling effectiveness, ASME Journal of Turbomachinery 122 (2000) 153–160 January.
[8] K. Kusterer, D. Bohn, T. Sugimoto, R. Tanaka, Double-jet ejection of cooling air for improved film cooling, ASME Journal of Turbomachinery 129 (4) (2007) 809–815.
[9] J.D. Heidmann, S. Ekkad, A novel anti-vortex turbine film cooling hole concept, ASME paper GT2007-27528, 2007.
[10] J.T. Bai, H.R. Zhu, C.L. Liu, Inside the channels of crisscross of cross-flow gas film cooling efficiency influence, Journal of Aerospace Power 23 (8) (2008) 1353–1358 (in Chinese).
[11] Fluent Inc., Fluent 6.3 documentation, Lebanon, NH, 2008.
[12] C.L. Liu, H.R. Zhu, J.T. Bai, Study on the physics of film-cooling effectiveness enhancement by the converging-expanding hole, Journal of Aerospace Power 23 (4) (2008) 598–604 (in Chinese).
[13] C.H.N. Yuen, R.F. Martinez-Botas, Film cooling characteristics of a single round hole at various streamwise angles in a cross flow, Part I: effectiveness, International Journal of Heat and Mass Transfer 46 (2) (2003) 221–235 January.
[14] G. Michael, A. Schulz, S. Wittig, Effect of crossflows on the discharge coefficient of film cooling holes with varying angles of inclination and orientation, Journal of Turbomachinery 123 (4) (2001) 781–787.